Numerical Investigation of Plasma Actuator Configurations for Flow Separation Control at Multiple Angles of Attack

Thomas K. West IV and Serhat Hosder
Missouri University of Science and Technology, Rolla, Missouri – 65409, USA
Corresponding Author E-mail: tkwgg3@mst.edu

Received date 9th July 2012; Accepted date 6th February 2013

Abstract
The objective of this study was to analyze the effectiveness of aerodynamic plasma actuators as a means of active flow control over an airfoil at multiple angles of attack under low Reynolds number conditions. Each angle of attack corresponded to two different flow separation mechanisms (i.e., laminar separation bubble (LSB) and fully turbulent flow separation at stall conditions). Detailed parametric studies based on steady and unsteady Reynolds Averaged Navier-Stokes simulations were performed for a NACA 0012 airfoil at a chord Reynolds number of 10^5 to investigate the influence of the number, the location, the imposed body force magnitude, and steady vs. unsteady operation of plasma actuators on flow control effectiveness. For LSB control, as much as a 50% improvement in the lift to drag ratio was observed. Results also show that the same improvement was achieved using unsteady or multiple actuators, which can require as much as 75% less time averaged body force compared to a single, steady actuator. For the stalled airfoil case, significant recovery in aerodynamic performance was observed for a single, steady actuator. However, for the stall conditions considered in this study, unsteady and multiple actuator configurations do not provide the same enhancement as a single, steady actuator, which may be due to the nature of the flow separation (turbulent, trailing edge separation). The results of both cases show that the optimum location of a plasma actuator would be just upstream of the separation location for maximum effectiveness. This highlights the usefulness of multiple actuator systems for flow control over a range of operating conditions as the separation location may be dynamic.

1. INTRODUCTION

In recent years, the area of active flow control techniques in aerodynamics has been a great topic of interest. Among these techniques is the aerodynamic plasma actuator. Plasma actuators have been shown to be effective in a variety of flow scenarios involving flow separation and boundary layer control [1]. Huang et al. [2] demonstrated separation control over low pressure turbine blades used in gas turbine engines at low Reynolds numbers (50,000 to 100,000) typical for high altitude cruise. Benard et al. [3] showed that plasma actuators could be used to improve free shear layer mixing at a nozzle exit achieved with significant enhancement of the jet spreading, jet core length reduction, and an increase in turbulent kinetic energy throughout the flowfield. Plasma actuators have also been used as devices for noise reduction. In a study performed by Thomas et al. [4], plasma actuators were used to study the plausibility of flow separation control over bluff bodies, in particular cylinders which are commonly found on aircraft landing gear, and are a source of noise during takeoff and landing. One of the most studied applications of plasma actuators is their application to airfoils for separation control in low Reynolds number flows [5,6,7] and was the focus of this study. The objective was to analyze the effectiveness of plasma actuators in providing flow separation control for improved aerodynamic performance over a NACA 0012 airfoil at a chord Reynolds number of 10^5 using computational fluid dynamics (CFD). Many practical aerodynamic applications exist for this Reynolds number including wind turbines, high altitude UAVs, micro-air vehicles, and some turbo-machinery applications.

With improvements in numerical modeling techniques and computational resources, an increasing amount of research has gone into the study of plasma actuators using numerical simulations. The biggest challenge with simulating plasma actuators remains to be modeling the behavior of the actuator, its effects on the surrounding flowfield, and the distribution of the plasma region. Many different numerical models have been developed as the ongoing research in the area of plasma actuators expands. Suzen et al.[1] made use of a model based on Maxwell's equations stating the body force produced by the plasma actuator is a function of the charge density and the strength of the electric field produced by the actuator. In the same study, the plasma distribution over the embedded electrode was modeled using half of a Gaussian distribution, which was stated to represent previous experimental results. This model is considered to be a high fidelity model that represents the performance of the actuator based on the physics. On the other hand, Aholt and Finaish [8] incorporated a body force source term into the Navier-Stokes equations. Even though this model was not based on the physics governing the actuator (i.e., the solution of Maxwell Equations), this simple, but useful, model was successfully used to demonstrate the effectiveness of using plasma actuators as a means of active flow control. This is the approach that was used in the current study for its computational efficiency and suitability for parametric studies.

In terms of simulating the flow around plasma actuators, many different methods have, again, been implemented. Because flow separation is an unsteady phenomenon and related to turbulence transition, only Large-Eddy Simulations (LES) or Direct Numerical Simulations (DNS) can accurately resolve the flow structure. Visbal et al. [9] has shown that the use of implicit LES simulations perform well when simulating the effects of plasma actuators on flowfields with large separation regions, such as the stall separation of an airfoil. However, LES and DNS methods are computationally very expensive, making less expensive Reynolds-Averaged Navier-Stokes (RANS) simulations with various turbulence models [8,10,11] an alternative to study the basic effects of plasma actuators, especially for aerodynamic design cases that involve active flow control.

Using steady and unsteady CFD simulations based on the solution of the RANS equations, the primary objective of this study was to demonstrate separation control with plasma actuators over a range of angles of attack, each corresponding to a different flow regime at low speeds. Due to the Reynolds number considered, the control of laminar separation bubbles at lower angles of attack was investigated, as well as fully turbulent separated flows at the stall angle of attack.

This study makes two main contributions to the field of using plasma actuators as a means of active flow control for airfoils. First and foremost is the demonstration of the use of plasma actuators across a range of angles of attack. One single actuator, at one location may not have the capability to control the entire flowfield ranging from downstream, laminar separation regions to the leading edge (or trailing edge) turbulent separation of a stalled airfoil as the separation location may be in a different location at each angle of attack. In light of this, the second major contribution is demonstrating the effectiveness of multiple plasma actuators. A multiple actuator configuration may provide a means of active flow control in a dynamic environment, at least in the instance when realistic voltage needs are required. In addition to the two main contributions, a simplified approach to relate the input parameters of the numerical simulation to the operating parameters of an actual plasma actuator was employed. The results of this study are, therefore, given in terms of actuator voltage and frequency, as these are the main input parameters for actual plasma actuator operation.

The following section describes the problem to be investigated in this study which includes a description of the types of flow separation of interest. In section 3, a brief description of the fundamentals of aerodynamic plasma actuators is given, followed by explanations of their possible configurations and modes of operation. Section 4 then provides the information regarding the numerical solution procedure and methodologies utilized in this study. This includes a description of the computational grid, the selected flow solver, turbulence modeling, and the numerical model of the plasma actuator. Section 5 then gives the results with in-depth discussion and explanations followed by a conclusion in section 6 which summarizes the findings of this study.

2. PROBLEM DESCRIPTION

At angles of attack less than that of the stall angle, it is possible for flow separation to occur, particularly at the low Reynolds number investigated in this study. Shen et al.[12] performed direct numerical simulations around a NACA 0012 airfoil at a chord Reynolds number of 10^5 illustrating the presence of flow separation due to the detachment of the laminar boundary layer from the airfoil surface as early as 4 degrees angle of attack downstream of the leading edge. This may occur when the laminar boundary layer encounters a strong adverse pressure gradient [8] or due to curvature changes of the surface as described by Shan et. al [12]. The separated shear layer, in some cases, may undergo a rapid transition to turbulent flow which could cause the shear layer to reattach to the surface, forming an attached turbulent boundary layer. This yields the development of a laminar separation bubble. It is important to note that the formation of this bubble may not occur at all angles of attack. If the angle of attack is too low, the pressure gradient will not be large enough to induce a detachment of the laminar boundary layer from the surface. On the contrary, if the angle of attack is too high the pressure gradient may be large enough such that laminar separation occurs, but without reattachment. The formation of this bubble, shown in Figure 1, can have an extremely detrimental effect on aerodynamic performance as the separation bubble causes an increase in the pressure drag on the airfoil [8]. One objective of this study was to investigate if plasma actuators have the ability to either delay or even prevent the formation of laminar separation bubble. This would allow for increased suction on the leading edge causing an increase in lift and would reduce the pressure (form) drag over the airfoil.

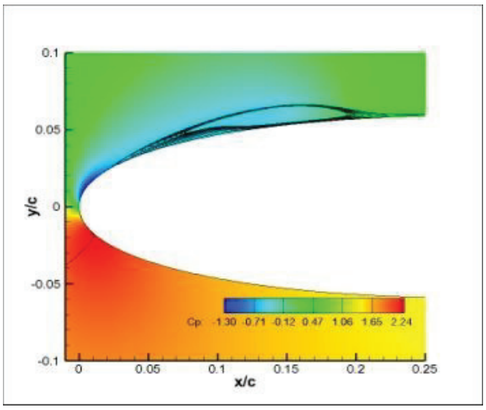

Figure 1. Leading Edge Laminar Separation Bubble at 8 Degrees Angle of Attack (Pressure Coefficient Contour with Streamlines)

At the stall angle of attack, a large-scale separation region occurs over nearly the entire upper surface of the selected NACA 0012 airfoil. This region of separation dramatically influences the lift and drag characteristics of the airfoil in a negative manner. For the given Reynolds number, it is assumed that the flow is fully turbulent at the stall angle, which was determined to be 15 degrees. This means that there is no longer an imposed laminar to turbulent transition region as with the previously discussed scenario. Physically, this represents a case in which the flow immediately transitions to turbulent flow upon reaching the airfoil, due to the large adverse pressure gradient. Figure 2 shows how the separation region expands with increasing angle of attack.

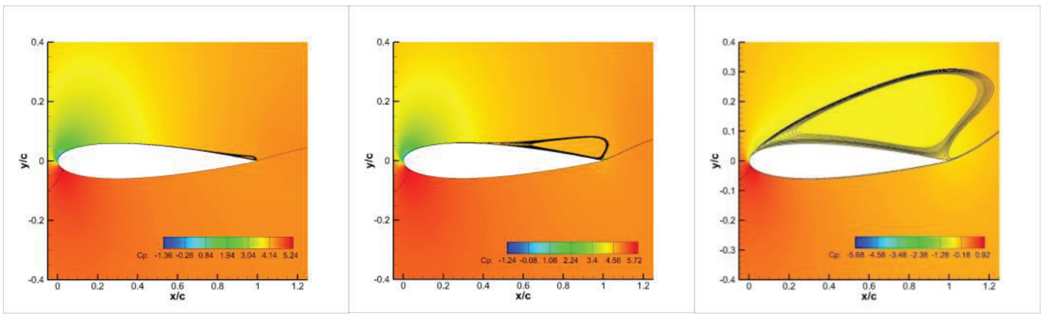

12 Degrees 14 Degrees 15 Degrees

Figure 2. Flow Separation Region Development from 12 to 15 Degrees Angle of Attack with Fully Turbulent Flow Assumption (Pressure Coefficient Contour with Streamlines Defining the Separation Region)

Prior to 15 degrees, with a fully turbulent flow assumption, the flow separation starts from the trailing edge, which begins to develop at about 12 degrees angle of attack and increases through 15 degrees where the separation region grows past the maximum thickness location (30% of the chord for this airfoil) and engulfs the entire upper surface. The objective of this portion of the study was to use aerodynamic plasma actuators to force the separation downstream such that separation region no longer covers the entire upper surface leading to an improvement in the lift-to-drag ratio.

3. PLASMA ACTUATOR DESCRIPTION, CONFIGURATIONS, AND OPERATION

3.1. Aerodynamic Plasma Actuators

The single dielectric barrier discharge (SDBD) plasma actuator [11] is a relatively simple device consisting of a pair of electrodes separated by a dielectric material, typically arranged in the asymmetric configuration shown in Figure 3. In experiments conducted by Corke et al.[5,6] the electrodes were made of a copper foil tape, while the dielectric material was made of a kapton film. Other dielectric materials can be used such as Macor, Teflon, or even glass. The primary differences between the materials are their breakdown voltages and ductility. The ductility affects the integration of the actuator, as those dielectrics with low ductility such as Macor cannot be easily integrated on curved surfaces [3]. In typical aerodynamic applications, one of the electrodes is exposed to the air, while the other is embedded in some surface, such as the skin on an aircraft wing, completely covered by the dielectric material.

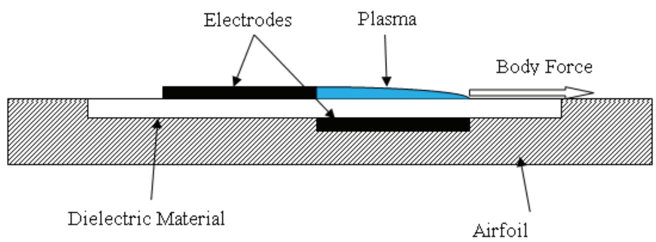

Figure 3. Schematic of a Single Dielectric Barrier Discharge Plasma Actuator

When an AC voltage is applied across the electrodes, and the frequency is large enough, the air ionizes in the region with the largest electric potential. As shown in Figure 3, this region is located above the embedded electrode, beginning near the edge of the exposed electrode. The ionized air, or plasma, in the presence of an electric field gradient, produces a body force on the ambient air [3], directed away from the exposed electrode, parallel to the dielectric material.

In order to ionize the air using the plasma actuator, it is required that a large, typically between 5 and 10 kV, AC voltage be applied across the electrodes, operating with an input frequency of 1-10 kHz [13]. Because of the large frequencies, plasma actuators can be regarded as "quasi-steady" devices, as these frequencies are typically well above the fluid response frequency [6]. Even with the large voltage demands, plasma actuators are relatively low power devices, operating around 2-40 Watts per foot of actuator span [5]. Enloe et al. [13] describe, in great detail, the electrodynamics governing plasma actuators.

Plasma actuators have many advantages over other flow control devices. First, plasma actuators can be used as an active flow control device. This means that they can be used in a time of need, and not in constant, uncontrolled use as with, for example, passive vortex generators [14]. One of the greatest advantages is that, when properly integrated, plasma actuators have almost no effect on the flow when in the off position as the exposed electrode is typically less than 0.1 mm thick. Also, from a mechanics stand point, plasma actuators have no moving parts, making them solid-state devices, which are much simpler than mechanical devices with potentially complex mechanisms.

3.2. Single vs. Multiple Actuator Configurations

In some cases, the use of a single plasma actuator as a means of flow separation control may not be possible for two primary reasons. The first involves the placement of the actuator with respect to the separation location. As the angle of attack changes, so does the structure and location of any separation. Multiple actuators placed at different locations may enable flow control over a range of angles of attack, by operating the actuator(s) at the optimum location and leaving the less effective actuators idle. This could allow for increased efficiency in terms of power usage. An objective of this study was to investigate the dependence on actuator placement for effective and efficient flow control for the two types of separation described in section 2 using the same set of actuators for both flow scenarios.

The second reason is due to the magnitude of the separation region and its response to the added momentum from a plasma actuator. An example of this would be flow separation at the stall angle of attack, which is strong and, after a perturbation, the fluid recovery time (the time it takes for a fluid to return to its original state after a perturbation) is extremely small. Here, the use of one actuator may delay the separation of the boundary layer, but if this delay is not sufficient, substantial flow separation may still ensue. The application of multiple actuators could be used to further delay the separation point of the boundary layer by providing a longer distance over which momentum is added to the flow. With this, it may also be possible to reduce the input voltage for each actuator in an array compared to a single, higher voltage actuator. One of the objectives of the current study was to investigate the plausibility of using an array of lower voltage plasma actuators to control the two flow separation cases of interest in this study.

3.3. Steady vs. Unsteady Operation

As mentioned previously, plasma actuators can be regarded as a "quasi-steady" device. This implies that if the actuator was operated continuously, the fluctuations due to the AC voltage are negligible. It has been shown that the use of a "pulsed" actuator can provide significantly greater aerodynamic performance enhancement, even beyond that of a steady state actuator for certain cases [9]. The pulsing effect of the unsteady actuator can generate large coherent vortices that could delay or even prevent separation. These structures intermittently bring high momentum fluid to the surface, helping the flow withstand the adverse pressure gradient without separation [6]. One tremendous advantage to using a pulsed actuator is that the power requirement may be less than that of a steady actuator, and the gain in aerodynamic performance could be the same, if not better than a steady actuator [5,6].

The actuator time dependency, or rather the actuation period and frequency, can be modeled based on the physical frequency of the fluid given by the Strouhal number, shown in Eq. (1) where L_{sep} is the length of the separation region and U_∞ is the free-stream velocity.

$$St = \frac{fL_{sep}}{U_\infty} \tag{1}$$

It has been shown that the optimum actuator frequency, , occurs when the Strouhal number is near unity [5,6,7,9]. After solving Eq. (1) for the frequency, a fundamental period can be determined using Eq (2).

$$T_f = \frac{1}{f} \tag{2}$$

This fundamental period can also be regarded as one actuation period. The fraction of this period that the actuator is operating is known as the duty cycle. For instance, if the duty cycle is equal to 1, this implies that there is no unsteady period during the operation of the actuator over one fundamental actuator period; or rather, this would be a steady actuator. On the other hand, if the duty cycle was 0, there would be no actuation over the fundamental period; or rather, the actuator would be in the off position. The relationship between the duty cycle, DC, and fundamental period is shown in Eq. (3), where T denotes the time that the actuator is on during one fundamental period. This is shown graphically in Figure 4 where the actuator behaves as a step function between the on and off position as a function of time.

$$DC = \frac{T}{T_f} \tag{3}$$

The duty cycle can also be interpreted another way. In terms of power, the duty cycle represents the power usage of an unsteady plasma actuator, compared to an actuator in steady operation. For example,

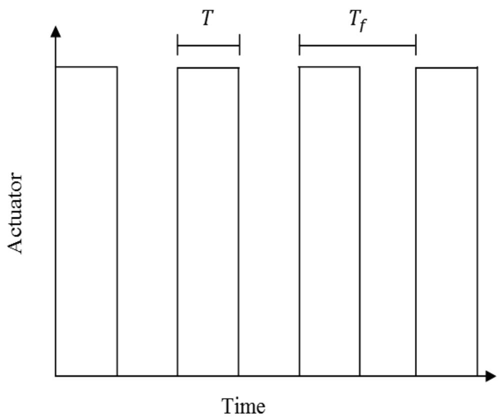

Figure 4. Graph of Actuator Unsteady Operation

an actuator operating with a 10% duty cycle uses 90% less power than a steady actuator over the same time period. For this study, a duty cycle of 50% was used for the unsteady actuator analysis as this has been shown to be adequate for aerodynamic control applications [9].

In the cases of the multiple actuator configurations, the actuators were operated such that the each was offset by one actuation period. For example, if actuator 1 is on from t=1.0 s to t=1.1 s, then actuator 2 was operated from t=1.1 s to t=1.2 s, and so on. The benefit of offsetting the actuators is that the influence of the body force propagates downstream with the flow. It will later be shown that the effect of the actuator is to push the separation location downstream making the use of offset actuators ideal to move the separation location as far downstream as possible.

4. NUMERICAL MODELING OF FLOWFIELD AND PLASMA ACTUATOR

4.1. Flow Solver

The computational fluid dynamics (CFD) code used in this study for the numerical solution of steady and unsteady RANS equations was the commercially available solver ANSYS FLUENT 12 [15]. Eq. (4) and (5) are the conservation equations for mass and momentum, respectively, that are solved numerically by the flow solver.

$$\frac{D\rho}{Dt} + \rho(\nabla \cdot V) = 0 \tag{4}$$

$$\rho\frac{DV}{Dt} = -\nabla P + \mu\nabla^2 V \tag{5}$$

Here, V is the velocity field, ρ is the fluid density, P is the pressure and μ is the dynamic viscosity. Note also that $\frac{D}{Dt}$ is the material or total derivative. The selection of FLUENT was made due to the various solution capabilities, including the ease of incorporating a model to represent the plasma actuators through the use of a user defined function (UDF). A UDF allows for additions and/or alterations to the flow solver and governing equations by compiling subroutines and linking them to FLUENT. The solutions for this study were obtained using the pressure based, segregated solver. Second order spatial discretization was applied for pressure and momentum, as well as the selected turbulence model. The absolute convergence requirement of all residuals was set to 10^{-6}. For pressure-velocity coupling, the SIMPLE method was implemented. To handle the transient flow discretization, a second-order implicit time marching scheme was implemented for time integration of the solution.

The convergence of each case was achieved by ensuring that each of the governing equations (mass and momentum) and the turbulence model equation converged to the prescribed absolute convergence requirement. For steady state cases, iterations were performed until the convergence requirement was met. For transient cases, convergence was achieved for each time step where the time step size was 0.01 seconds. Lift and drag data was then extracted from the converged cases. This is direct for steady flow cases as the lift and drag are a singular value. However, unsteady cases exhibit periodic behavior of the lift and drag coefficients. In order to determine the lift and drag for these cases, a mean of each is taken when the periodic motion is approximately centered about a single value with constant amplitude (i.e. after the flow has fully developed.)

4.2. Geometry and Computational Grid

A symmetric NACA 0012 airfoil with a 1 meter chord length was the geometry of interest for this study. The geometry and computational grid were both constructed using a hyperbolic C-type grid generator [16] developed for constructing grids around airfoils. The grid size was 20 chord lengths from the origin, located at the leading edge of the airfoil, in every direction while the wall spacing to the first grid point from the airfoil surface was 2.3×10^{-5} m. This corresponds to a y+ value less than one for the selected Reynolds number. The objective was to completely resolve the turbulent boundary layer, including the viscous sub-layer, without the use of wall functions. The dimensions of the grid used in this study were 999x200, where the first number corresponds to the number grid lines in the streamwise direction and the second is the number of gridlines in the direction normal to the wall. Note that grid convergence was verified for this grid size using two coarser grid levels at angles of attack ranging from 0 to 16 degrees [17]. Figure 5 depicts various aspects of the computational grid.

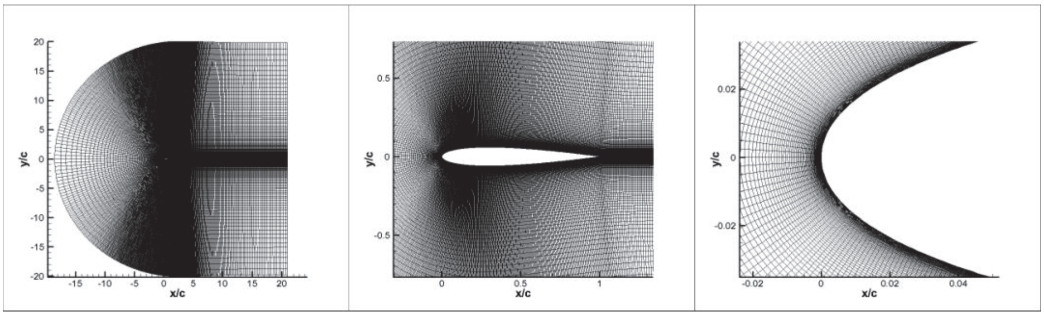

a) Full Grid View b) Airfoil View c) Near-Wall LE Region

Figure 5. Computational Grid around the NACA 0012 Airfoil

4.3. Boundary Conditions

There are three main boundaries of the computational grid, shown in Figure 6. Two of these are the farfield boundaries. The left-hand side, top edge, and bottom edge were modeled as velocity inlets while the right edge of the grid was set as an outflow boundary. These boundary conditions are suitable for the low speed, incompressible flow analyzed in this study. The other boundary is the airfoil surface, which was modeled as a no-slip wall boundary. The inlet conditions were set such that free stream flow had a chord Reynolds number 100,000. Sea level density (1.225 kg/m^3) and dynamic viscosity (1.7894×10^{-5} kg/m-s) were used as the free-stream air properties. This corresponds to a free-stream velocity of 1.46 m/s.

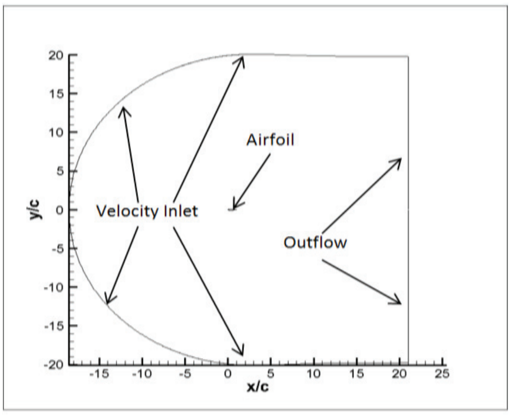

Figure 6. Computational Grid Boundaries

4.4. Modeling of Turbulence and Turbulent Flow Transition

FLUENT 12 has a wide variety of turbulence models readily available, with an array of settings and correction factors. For this study, the one equation Spalart and Allmaras [18], Eddy-Viscosity model was employed to simulate the turbulent flow.

Because of the use of the Reynolds Averaged Navier-Stokes (RANS) equations by the FLUENT solver, special arrangements had to be made in order to model the laminar separation bubble formed at low angles of attack. Simple RANS modeling lacks the ability to accurately predict laminar to turbulent transitions. It is typical that when using RANS modeling, the transition location be specified by the user. In FLUENT, this was done by partitioning the computational grid into to two zones. The location of the partition varies depending on the location of the laminar separation, which is analogous to the angle of attack to the airfoil. The partition is placed at the location that causes the greatest aerodynamic performance loss while still forming the separation bubble for each selected angle of attack. Although with this approach, the transition is imposed at a single point, this method gives a flow structure consistent with the physics associated with the laminar separation bubble formation phenomenon [19] (See Figure 1). This is also the procedure used by Aholt and Finaish [8] as part of their study of the control of laminar separation bubbles. In order to relax this assumption, higher fidelity computation methods such as Large-Eddy Simulations (LES), Detached-Eddy Simulations (DES), or Direct Numerical Simulations would be necessary. However these methods are computationally much more expensive than RANS modeling.

4.5. Plasma Actuator Model

It is well understood that plasma actuators impart a body force on the flow. This is synonymous to adding momentum to the flow in a prescribed region. This region is approximately where the plasma is created by the actuator. To model a plasma actuator in FLUENT, a UDF was compiled into the solver, adding a momentum source term to the governing equation for momentum shown in Eq. (6).

$$\rho \frac{DV}{Dt} = -\nabla P + \mu \nabla^2 V + \rho f \tag{6}$$

$$\rho f = F_b = \rho_c E \tag{7}$$

Here, V is the velocity field, ρ is the fluid density, P is the pressure, μ is the dynamic viscosity and ρf, shown in Eq. (7), is the body force per unit volume of plasma created by the plasma actuator [1,6,11]. In this relation, ρ_c is the charge density and E is the electric field produced by the plasma actuator.

This source term was restricted to the area designated as the location and size of the plasma region of the actuator. Experiments [5,6] have shown that the actuator electrodes can be comprised of thin foil tape and for electrodes in an asymmetric configuration, the size of the plasma region is approximately the same height or thickness as the exposed electrode. However the length of the plasma is highly depended on the ambient conditions in that as the pressure decreases, the length of the plasma produced by the actuator increases in the chordwise direction. This has been demonstrated through experimental by Nichols and Rovey [20]. For this analysis, the length of the plasma region was taken to be the same length as the embedded electrode. Given the sea level free stream conditions at a very low speed, low pressure and density effects should be minimized in the plasma actuator modeling. The dimensions of the plasma region were chosen to be 10 mm long by 0.1 mm thick which represents the relative size of the foil tape used in previous experiments.

For design purposes, it is necessary to determine the input voltage and frequency of the plasma actuators used in this study. As the input into the UDF is a force per unit volume and the dimensions of the plasma region are specified, a relationship is needed to determine such information. Porter et al.[21] performed an experiment to develop relationships between the force per unit length and the input frequency and voltage. The results of the current study are presented with a fixed input frequency of 5 kHz, and a linear relationship between the force per unit span of the actuator and the input voltage. The force per unit span changes with the input voltage using Eq. (8).

$$F_B = 3.26\,V - 17.32 \tag{8}$$

Here, F_B is in mN/m and V is in kV. Note that in the study by Porter et al.[21], data was only taken up to about 10 kV. The approximation in Eq. (8) should be sufficient for providing insight into the requirements for a physical system that utilizes plasma actuators in the manner demonstrated in this study. Note that frequency of the unsteady operation of the actuator is much less than the operational frequency of the actuator. In this study, the highest frequency analyzed was only 20 Hz, where the assumed operational frequency of the actuator is 5 kHz.

5. RESULTS AND DISCUSSION

5.1. Laminar Separation Bubble (LSB) Control

In this portion of the study, the flowfield at 8 degrees angle of attack was analyzed. Three plasma actuators located at 2, 4, and 6 percent of the chord length were employed with varying body force magnitudes, or rather, voltage inputs. (Recall that the input frequency is fixed at 5 kHz for the experimental relationship used.) The minimum voltage used was 5.62 kV which corresponds to a force of 1 mN/m. Porter et al.[21] noted that there is a threshold voltage of 5.31 kV where no plasma is generated. Table 1 and Table 2 give the results for the lift to drag ratios (L/D) of the performed parametric study at 8 degrees angle of attack. The parameters were the actuator configuration (single or multiple), operation mode (steady or unsteady), and the input voltage.

Additionally, the same parametric analysis was performed at 10 degrees angle of attack to illustrate how the same set of actuators performs when the separation location has changed. The results and conclusions were found to be similar compared to 8 degrees angle of attack. Results for 10 degrees angle of attack, while not shown below, are given by West [17].

5.1.1. Investigation of Flow Control with a Single, Steady Actuator

The first scenario analyzed involved the use of a single, steady-state actuator. The three actuators were operated at three different input voltage levels to illustrate the effect of the strength of the body force on LSB control. Pressure coefficient contours with stream traces on the upper surface in the vicinity of leading edge are shown in Figure 7. For the case with no actuator at 8 degrees angle of attack, from Table 1, the lift to drag ratio (L/D) was about 21.91. By inspection of Figure 7, it can be seen that the plasma actuator has the ability to drastically reduce the size of the separation region. Evaluation of the L/D results in Table 1 shows that there is as much as a 45% improvement in L/D when using a single, steady actuator.

This is a significant improvement in aerodynamic performance. The reduction in the size of the separation region allows for a decrease in pressure drag as well as an improvement in the pressure distribution with an increase in the suction near the leading edge. Note that these results are consistent with those observed by Aholt and Finaish [8] where a 60% improvement in L/D was found when using a single, steady actuator to control an LSB over an elliptical airfoil.

Table 1. Parametric L/D Results for Laminar Separation Bubble Control at 8 Degrees Angle of Attack with a Single Plasma Actuator

8 Degrees	Actuator Location		
V (kV), Duty Cycle	2 % c	4 % c	6 % c
No Actuator	21.91	21.91	21.91
5.62, DC=50%	30.31	22.72	21.81
5.62, Steady	27.09	22.70	21.71
5.93, DC=50%	32.32	25.98	22.06
5.93, Steady	29.33	24.96	21.92
6.54, DC=50%	32.65	32.57	23.38
6.54, Steady	30.89	31.67	31.36

Table 2. Parametric L/D Results for Laminar Separation Bubble Control at 8 Degrees Angle of Attack with Multiple Plasma Actuators

8 Degrees	Actuator Location		
V (kV), Duty Cycle	2 & 4 % c	2 & 6 % c	4 & 6 % c
No Actuator	21.91	21.91	21.91
5.62, DC=50%	31.16	30.85	22.79
5.62, Steady	29.69	27.55	22.76
5.93, DC=50%	32.69	32.55	31.14
5.93, Steady	31.11	31.28	31.40

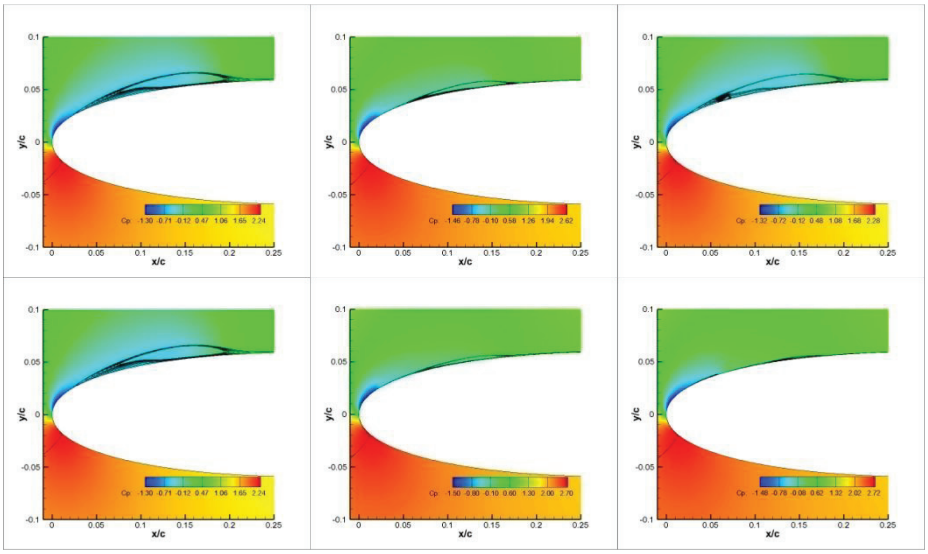

No Actuator 2% c 6% c

Figure 7. Pressure Coefficient Contours with Streamlines for One Steady State Actuator at 8 Degrees Angle of Attack, V = 5.93 kV Top, V = 6.54 kV Bottom (V = Input Voltage with 5 kHz Input Frequency)

The images above also illustrate the importance of the location of the actuator. Because of the large magnitude of the source, the 6.54 kV cases appear to be independent of the actuator location. However, at the lower force level, it can be seen that as the actuator moves downstream, its effectiveness decreases. In fact, at the 6% chord location, the flow behaves as if there was no flow control device present at all. From Table 1, the results are similar between the 5.93 kV and the 5.62 kV cases in that actuator location determines effectiveness. Improvement in L/D by the 5.93 kV actuator is greater due to the increased force magnitude over the 5.62 kV actuator case.

These results help to illustrate, physically, how the plasma actuator modifies the near-wall flowfield. Because of the body force near the wall, the flow is being accelerated near the wall, preventing separation from occurring. If the actuator is placed just before the point at which the separation of the boundary layer is anticipated, then the separation can be delayed, or even prevented. On the contrary, if the actuator is placed downstream of the separation point, the flow entrainment may not be substantial enough to reattach the flow. For this case, it can be seen that the actuator located at 2% of the chord length provides the most improvement in aerodynamic performance for the 5.93 kV input. However, the separation bubble is smaller for the 6.54 kV input when the actuator is located at 4% of the chord. At the higher force magnitude, the flow is being entrained near the wall, ahead of the actuator. This is preventing the separation from actually occurring until downstream of the actuator. By this time, the boundary layer only has a small time period before the transition to turbulent flow forces reattachment.

Figure 8 illustrates the magnitude of the pressure recovery achieved with a plasma actuator. This plot compares the surface pressure distribution of the airfoil without a plasma actuator to the case where there is one actuator located at 4% of the chord with an input voltage of 6.54 kV. Because of the added momentum near the leading edge of the airfoil, the suction on the upper surface spikes dramatically with over a 25% increase in the pressure coefficient near the leading edge. It can be seen that for this case the actuator does not entirely eliminate the separation bubble. However, the addition of the momentum near the wall delays the separation of the boundary layer enough such that there is very little time for the detachment distance of the boundary layer to increase before transitioning to turbulent flow and reattaching. Overall, there is about an 8% increase in lift and a 25% decrease in drag. Actually, the decrease in drag is quite interesting. The plasma actuator causes a 50% decrease in pressure drag. This can be explained by the reduction in the size of the separation bubble. The interesting part is the skin friction drag, which actually increases over 50%. The drag value components are shown Table 3. While

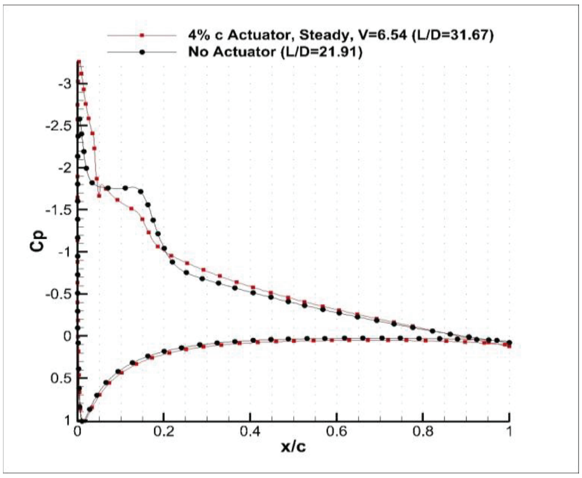

Figure 8. Surface Pressure Coefficient Distribution with and without a Single Plasma Actuator 8 Degrees Angle of Attack

the skin friction component of the drag is small for the uncontrolled case, the two drag components are nearly the same when the actuator is on as the contribution of each is about 50% of the total drag. Note that these results are only for this specific case. In the cases when the actuator does not significantly decrease the bubble size, the skin friction drag will be much less than the pressure drag component.

Table 3: Drag Component Values at 8 Degrees Angle of Attack for No Actuator and for a Single Actuator at 4% c, V = 6.45 kV

Actuator	Pressure Drag	Skin Friction Drag	Total
No Actuator	0.02658	0.00672	0.03330
4% c Actuator	0.01375	0.01147	0.02522

5.1.2. Investigation of Flow Control with a Single, Unsteady Actuator

In an effort to reduce the power consumed by the actuators, another mode of operation was considered. As mentioned earlier, it has been shown that the use of an unsteady or pulsed actuator can improve aerodynamic characteristics as much as, or even more than that achieved from a steady state actuator [5, 6, 9]. Figure 9 shows a time sequence of the effect of the unsteady actuator. Here, a periodic vortex shedding process is occurring. As the laminar separation bubble is forming, it is quickly forced to separate from the surface before developing into a large bubble. This can be seen as a kind of bursting effect. Due to the similarity between the scenarios involving unsteady actuators, only one example is given. As long as the vortex shedding is present, all that changes between different actuator locations and strengths is the size of the vortex that is shed. This means that a larger vortex will result in a greater loss in aerodynamic performance, but still may be better than a scenario where no control is present. This is evident in Figure 10. Because the drag is not as low for the 4% chord actuator compared to the 2% chord actuator, this suggests that the vortex being shed is larger for the 4% chord actuator. Note that in some cases, the actuator may have little or no effect on the separation region, as with the 6% chord actuator, shown in Figure 10. Similar to the steady actuators, this is due to the actuator placement with respect to the separation location. Placement of the plasma actuator is crucial, in that is must be located just upstream of the point of separation for the most efficient and effective flow control.

Also from Figure 10, note the improvement in the drag from the 2% chord unsteady actuator compared to the steady actuator at the same location. This is nearly a 10% improvement over the steady actuator. Table 1 shows that in every case, a single, unsteady actuator outperforms a single, steady actuator with the same input voltage. Because of the selected duty cycle of 50%, this implies that in every case, about 50% less time averaged body force, at a lower input voltage, is required to provide

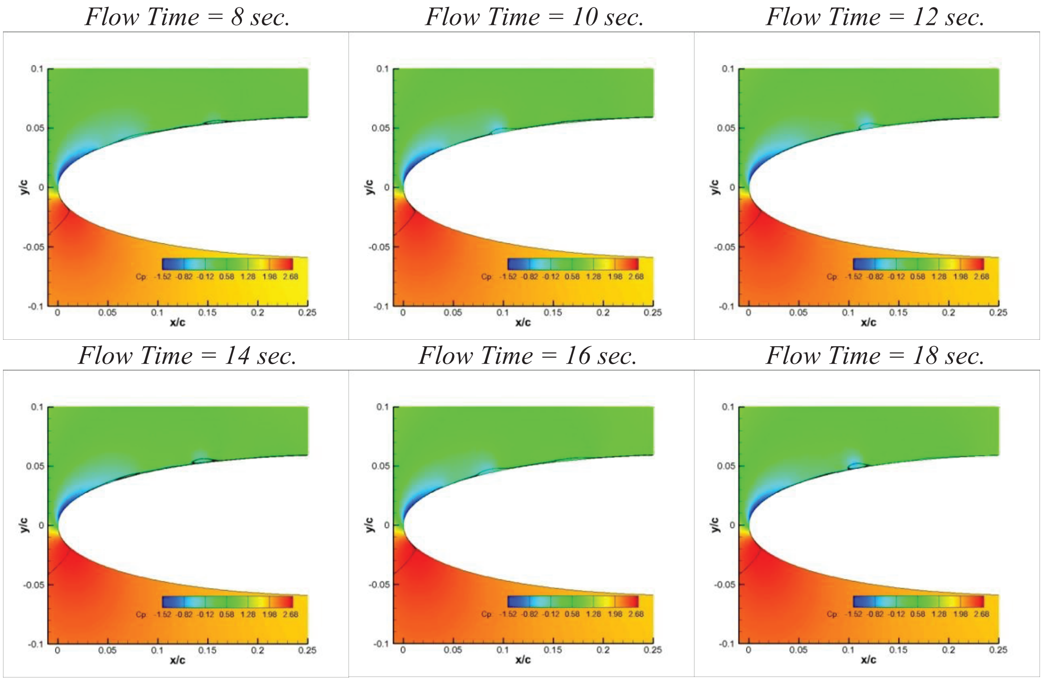

Figure 9. Time Sequence of Pressure Coefficient Contours with Streamlines at 8 Degrees Angle of Attack with One Unsteady Actuator at 4% c, V = 6.54 kV kV, DC = 50%

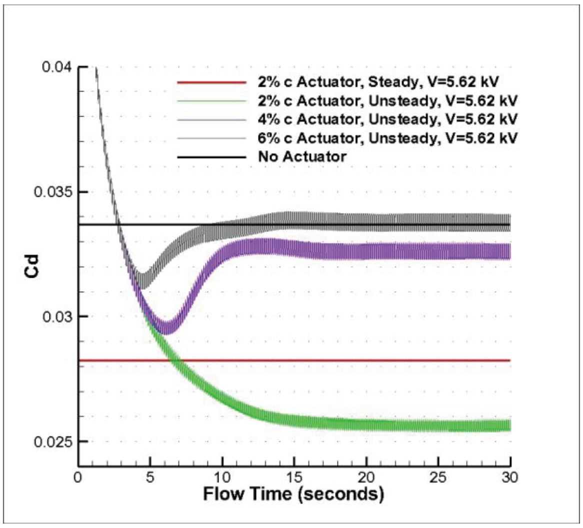

Figure 10. Drag Coefficient vs. Flow Time for a Single, Unsteady Actuators at 8 Degrees Angle of Attack, V = 5.62 kV, DC = 50%

the same, if not better control over the steady actuator. Refer to section 3.3 for the explanation of why unsteady actuators provide improved control over steady actuators.

5.1.3. Investigation of Flow Control with Multiple, Steady Actuators

Multiple actuators may offer a substantial gain in efficiency and control potential over a single actuator. Figure 11 shows a sample of the results of using two steady state actuators at 8 degrees angle of attack. Here, the actuators were being operated at lower input voltages than that of the single actuator cases, as this is one of the goals of using multiple actuator systems. Note that the same three actuators are still in use (2, 4 and 6% chord), in all possible combinations of two actuators. Refer to Table 2 for a complete listing of the results.

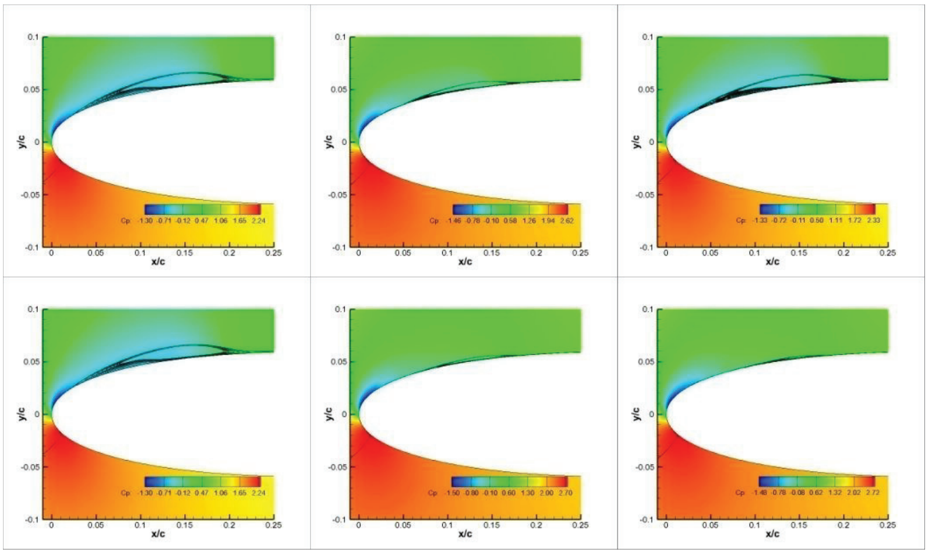

No Actuator 2 & 4% c 4 & 6% c

Figure 11. Pressure Coefficient Contours with Streamlines for Two Steady State Actuators at 8 Degrees Angle of Attack, V = 5.62 kV each Top, V = 5.93 kV each Bottom

As with the single actuator, the effects of the surface body force can be observed from the stream traces above. The separation point is pushed downstream, reducing the size of the separation bubble. With multiple steady actuators, the total body force acts as if it were an additive resultant from the two actuators. In general, if the actuators are close together, as in these cases, this statement will likely hold true. It may actually be difficult to discern between using one actuator or two, especially in the case when the fluid recovery time (the time it takes for a fluid to return to its original state after a perturbation) is large enough such that no separation occurs between the actuators.

5.1.4. Investigation of Flow Control with Multiple, Unsteady Actuators

Using the same actuator configurations as in the multiple, steady state actuator cases, the actuators were operated in an unsteady mode. Recall that multiple, unsteady actuators are operated just out of phase. Because of the 50% duty cycle used in this study, there was always one actuator operating at a given time. For the 8 degree angle of attack case, multiple, unsteady actuators provide nearly the same aerodynamic improvement as the cases with a single, unsteady actuator with the same body force over the same period of time. Also, because the actuators are so close together, the fluid behaves as if there is one steady actuator present on the surface of the airfoil. With a single, higher voltage actuator, the influence of the actuator reaches nearly the same distance downstream as the two unsteady actuators at a lower input voltage and gives the impression of nearly steady actuation. This holds true because there is no separation occurring between the actuators.

Note that for cases involving multiple, unsteady actuator configurations the same vortex shedding phenomenon is occurring similar to the cases with a single, unsteady actuator. Figure 12 shows an example of this at 8 degrees angle of attack as compared to having no actuator and a single, steady actuator of with the same time averaged body force magnitude. Notice that the 4% and 6% actuator chord array has a significantly higher drag than the other two configurations. As with the single, unsteady actuator cases, this is because the size of the vortex being shed is much larger than the other two configurations. Similar to all of the other actuator configurations discussed, this is related to the placement of the actuators with respect to the separation region. The 4% and 6% actuators lie inside the separation region and, with an input voltage of 5.62 kV each, the flow is not being entrained enough to prevent separation from occurring upstream of the 4% actuator. Due to the unsteadiness caused by the pulsing actuators, the described vortex shedding process is in place. However, in this case, only a portion of the separation bubble is being shed. The initial separation upstream of the 4% actuator is not being prevented or even suppressed. The reduced voltage input associated with the use of multiple, unsteady actuators is similar to that observed with a single, unsteady actuator. This means that as little

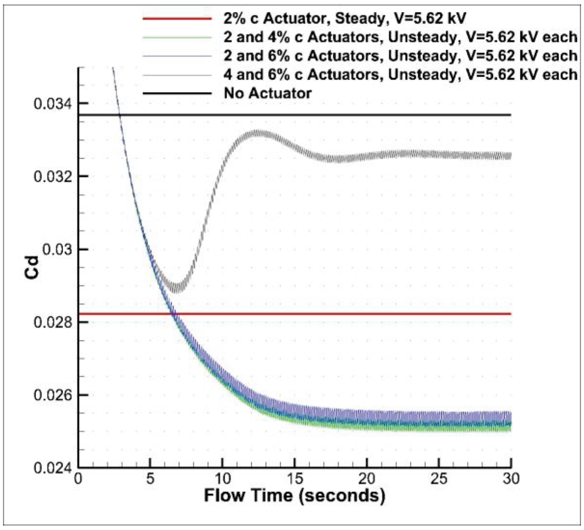

Figure 12. Drag Coefficient vs. Flow Time for Multiple, Unsteady Actuators at 8 Degrees Angle of Attack, V = 5.62 kV each, DC = 50%

as 25% of the total body force magnitude is necessary to provide the same enhancement using a single, higher voltage steady actuator.

5.1.5. Summary of the Results

The Effect of Plasma Actuator Location: For the lower input voltage, steady state actuators and all of the unsteady actuator arrangements, actuator placement dominates the effectiveness of the actuator(s). An actuator must be located just upstream of the separation location in order to have a substantial influence on the separation bubble. Here in lies the advantage/need of using multiple actuator systems. In this study, only one angle of attack was examined. If the angle of attack was reduced to five or six degrees, the separation location would be downstream [12] enough that the 2% chord actuator may not be as effective, and the 6% chord or even a further downstream actuator would be ideal. This reduced effectiveness in 2% chord actuator is due to the added momentum being dissipated before reaching the separation location. A similar trend may be observed for an actuator placed at the leading edge. The further the actuator is from the separation location, the less effective it is as a means of flow control.

The Effect of Steady vs. Unsteady Operation: Because the critical factor in implementing plasma actuators as a feasible, active flow device will likely be the input voltage, it is critical to reduce the required input in any way possible. This is where the use of unsteady actuators shows significant promise. From Table 1, notice that for a 6.54 kV, steady actuator at the 2% chord location, L/D = 30.98 whereas with a 5.93 kV, unsteady actuator (DC = 50%) at the 2% chord location, L/D = 32.32. This is an improvement over the steady actuator at 25% of the body force magnitude. It can be seen from Tables 1 also that, in general, unsteady actuators appear to always outperform steady actuators at the same time averaged body force magnitude.

The Effect of Multiple Plasma Actuators: The primary advantage of the multiple actuators is that, because of the dependence on the placement of the actuator, multiple actuators can give a wider range of control in an instance when the separation location is moving. The use of multiple actuators can also yield significant improvements over a single, high voltage actuator with lower input voltages per actuator. However, in terms of the total body force, the same aerodynamic performance enhancement gained from multiple actuators can be achieved using a single actuator at the same time averaged force magnitude and operational model (steady or unsteady.) This is because of the spacing of the actuators. The actuators used here were close together, which is necessary because of the size of the studied separation region. Regardless, the same trend still holds true that, as with the single actuators, unsteady operation of multiple actuators outperforms steady operation of multiple actuators for the same time averaged body force magnitude.

5.2. Flow Separation Control at Stall Angle of Attack

In this portion of the study, 15 degrees angle of attack was the angle of interest. At the selected Reynolds number (10^5) in this study, 14 degrees was the highest achievable angle of attack after which substantial separation and stall conditions were observed. At this angle, only a small region of trailing edge separation exists, which has little effect on the aerodynamic performance of the airfoil. At 15 degrees, the separation proceeds to cover nearly the entire upper surface of the airfoil, which severely compromises its lift and drag characteristics (Figure 2).

It is important note the type of separation observed for the NACA 0012 airfoil and flow conditions used in this study. At 15 degrees angle of attack, with a fully turbulent flow assumption, the flow separation originates in the trailing edge region. It will be shown that even after pushing the large trailing edge separation back downstream with plasma actuation, a small trailing edge separation region still remains, which appears to be stable in time.

Control of trailing edge separation may be different than what has been studied in previous literature as most of those cases focus on the control of leading edge separation with actuators placed in the leading edge region [6, 9]. The primary objective of the turbulent separation control investigated in this study is to force the separation region downstream as far as possible (i.e., to reduce the extent of the size of the separation region). Just moving the separation back past the maximum thickness of the airfoil will greatly improve the suction on the upper surface, which enhances the lift. An improvement in the drag will come from forcing the separation region as far downstream as possible and reducing the separation zone size, which greatly improves the pressure drag on the airfoil. As shown for the LSB control cases, increasing the body force magnitude to reduce the separation zone size also increases the skin friction drag. However, at the stall condition, the pressure drag component is significantly larger than the skin friction drag component making the increase in skin friction drag due to the addition of momentum near the wall negligible.

Table 4 and Table 5 give the results of the performed parametric study. Note that the parameters studied were the same as in the previous section. Also, the same 2, 4 and 6% chord actuators used in the previous chapter are used in this portion of the study with all of the same actuator configurations. The purpose of this is to demonstrate the control of both types of flow separation with the same set of actuators. However, the minimum voltage analyzed is higher than in the LSB control study. In this section, a minimum voltage of 7.77 kV was used as this is the voltage where flow control with either a single, steady or unsteady actuator was not possible. This is shown in Table 4. At the lowest voltage, the single, unsteady actuator cannot suppress the separation region.

5.2.1. Investigation of Flow Control with a Single, Steady Actuator

Figure 13 shows the pressure coefficient contours with streamlines for the cases with a single plasma actuator. It is important to note that the body force magnitude for these cases is as much as eight times higher than what was used as the highest voltage for the laminar separation bubble cases. This is expected as the separation at this angle of attack is larger, stronger, and much more stable making it more resistant to perturbations. For the case with no actuator, L/D = 3.18, as given is Table 4. From the images in Figure 13, the effect of the actuator on the separation region can clearly be seen. The

Table 4. Parametric L/D Results for Fully Turbulent Separation Control at 15 Degrees Angle of Attack with a Single Plasma Actuator

15 Degrees	Actuator Location		
V (kV), Duty Cycle	2 % c	4 % c	6 % c
No Actuator	3.18	3.18	3.18
7.77, DC=50%	3.95	3.23	3.20
7.77, Steady	15.73	12.30	11.30
10.22, DC=50%	14.47	12.24	11.61
10.22, Steady	20.92	16.52	15.17
15.13, DC=50%	18.76	15.90	15.56
15.13, Steady	25.85	20.84	19.24

Table 5. Parametric L/D Results for Fully Turbulent Separation Control at 15 Degrees Angle of Attack with Multiple Plasma Actuators

15 Degrees	Actuator Location		
V (kV), Duty Cycle	2 & 4 % c	2 & 6 % c	4 & 6 % c
No Actuator	3.18	3.18	3.18
7.77, DC=50%	14.83	14.30	12.09
7.77, Steady	18.59	18.43	15.09
10.22, DC=50%	20.03	19.23	15.83
10.22, Steady	22.30	22.64	18.30

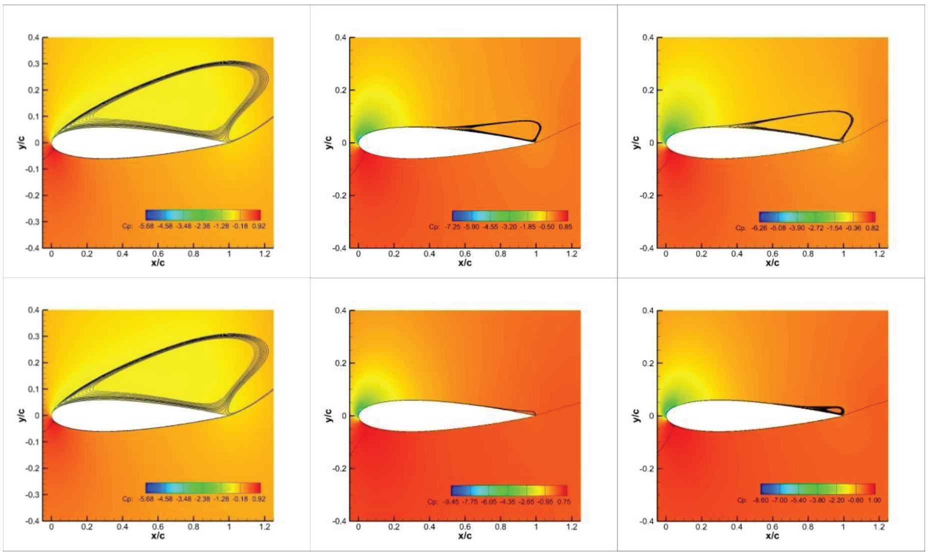

Figure 13. Pressure Coefficient Contours with Streamlines for One Steady State Actuator at 15 Degrees Angle of Attack, V = 7.77 kV Top, V = 15.13 kV Bottom

momentum added to the flow from the actuator forces the separation region downstream towards the trailing edge, reducing its size. From Table 4, even the worst case below (6% chord actuator with V = 7.77 kV) gives great improvement to the aerodynamic performance of the airfoil with L/D = 11.61. By forcing the separation region downstream past the maximum thickness, the suction on the leading edge increases significantly, such that the lift increases by almost 70%. The 2% chord with an input of 15.13 kV provides an L/D = 25.85 which is achieved by the massive increase in suction on the leading edge and the addition of near wall momentum that travels downstream fast enough to force the separation bubble almost completely to the trailing edge of the airfoil. Note that the 15.13 kV input value is above the maximum value used to develop the relationship for the actuator force as a function of the input voltage provided by Porter et. Al [21]. This value has been extrapolated from the data. It carries much uncertainty and may not be feasible in a real application.

Notice that in the cases with an input of 15.13 kV the size of the separation bubble is relatively the same between all three cases. The separation region for the 4% and 6% actuators is slightly larger, but not substantially. This might suggest that the L/D ratio is approximately the same. However, they are not as the L/D ratio of the 2% actuator is actually 35% higher than the ratio for the 6% actuator. Figure 14

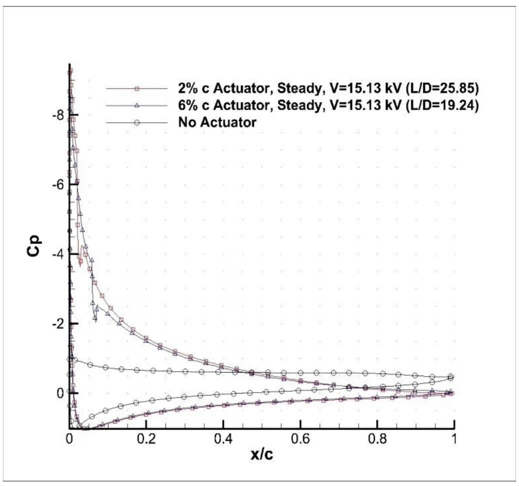

Figure 14. Surface Pressure Coefficient Distribution with and without a Single Actuator at 15 Degrees Angle of Attack

illustrates why this is so. From this figure, notice the suction increase on the upper surface. The pressure coefficient is about 12% lower for the 2% case. This provides about a 6% increase in lift. The remainder of the difference in the two L/D ratios then must come from the difference in drag. From Figure 13, it can be seen that the separation region is slightly smaller for the 2% cases compared to the 6% cases which accounts for the drag difference. Note that the 4% chord actuator cases are all between the 2% and 6% chord actuator results.

5.2.2. Investigation of Flow Control with a Single, Unsteady Actuator

For a single, unsteady actuator, the results are quite different when compared to the laminar separation bubble cases. Previously, the unsteady actuators induced a periodic vortex shedding process preventing the separation from growing to a stable, full size separation bubble. However, for the turbulent separation at stall conditions, this same phenomenon is not observed. Figure 15 shows a time sequence for a single, unsteady actuator. Notice that the separation region never detaches from the surface of the airfoil. What is seen is the separation generated by the trailing edge swelling, then deflating periodically. Figure 16 shows a plot of the drag coefficient versus the flow time for this case, which confirms the behavior of the separation region. In light of this, single, unsteady actuators do not perform as well as single, steady actuator. For a 2% chord, unsteady actuator with a 15.13 kV input, L/D is about 12% less than a steady actuator at the same location with the same time averaged body force magnitude with (V = 10.22 kV.)

For all studied cases, the unsteady actuators do not perform as well as steady actuators, which is not similar to the trend observed for the control of laminar separation bubbles. This is because there is always a region of separation attached to the airfoil surface which reduces the aerodynamic performance of the airfoil. The unsteady actuator does not provide a continuous force to suppress the separation coming from the trailing edge of the airfoil. The time between pulses of the actuator may be allowing for the separation region to recover slightly. This explains the lack of performance compared to steady actuator cases. Note, however, that there is still significant aerodynamic improvement when compared to the uncontrolled case.

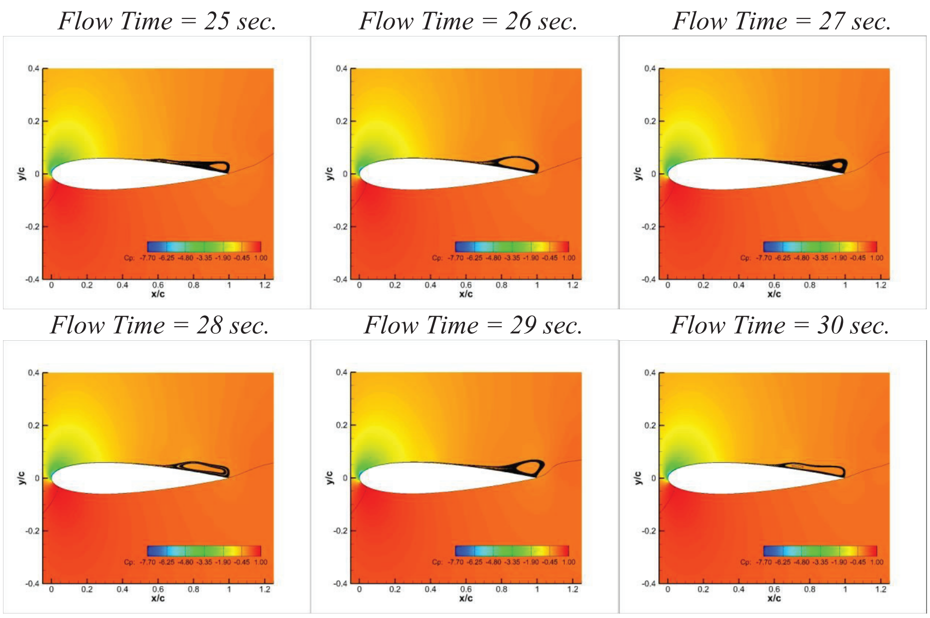

Figure 15. Pressure Coefficient Contours with Streamlines at 15 Degrees Angle of Attack for One Unsteady Actuator at 2% c, V = 15.13 kV kV, DC = 50%

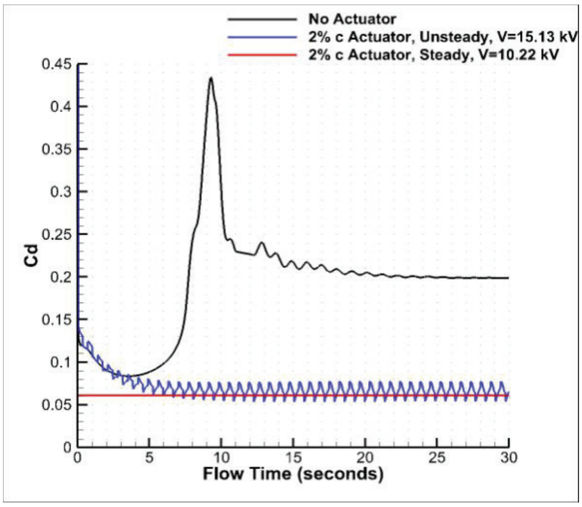

Figure 16. Drag Coefficient vs. Flow Time for a Single, Unsteady Actuator at 15 Degrees Angle of Attack, V = 15.13 kV, DC = 50%

5.2.3. Investigation of Flow Control with Multiple, Steady Actuators

The results for the cases with multiple, steady actuators are quite similar to the cases involving a single, steady actuator in terms of decreasing the size of the separation region. This is due to the fact the effect of multiple actuators is additive with regards to the total body force. Actuators with 10.22 kV input produce a force of about 16 mN/m. With two actuators, this implies that there is a total of 32 mN/m produced by the pair. This corresponds to an input voltage of 15.13 kV for a single actuator which was the highest voltage analyzed for a single actuator. Figure 17 gives the pressure contours with stream traces for the multiple, steady actuator cases. Table 5 shows that the best cases (highest L/D) are ones with actuators at 2% and 4% of the chord each with a 10.22 kV input. Comparing this case to the single 2% chord actuator case a 15.13 kV input shows that there are some slight differences. The L/D ratio is about 16% higher for the single actuator case. With regards to the lift, the suction near the leading edge is not as substantial with the lower voltage actuators and therefore the lift is not as high when compared

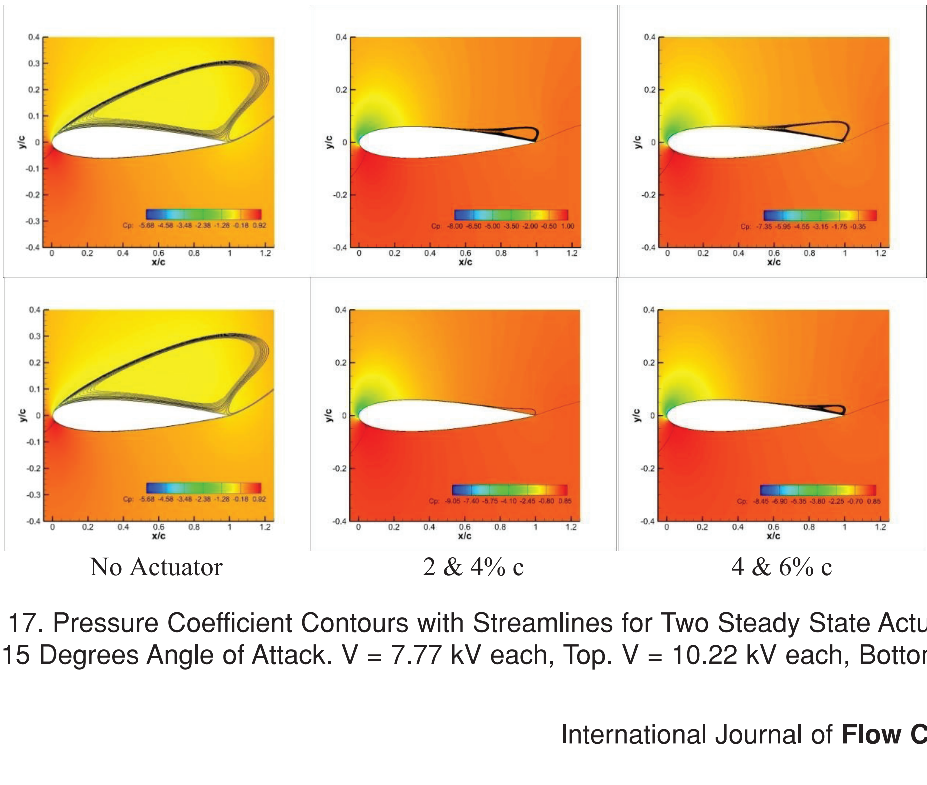

Figure 17. Pressure Coefficient Contours with Streamlines for Two Steady State Actuators at 15 Degrees Angle of Attack. V = 7.77 kV each, Top. V = 10.22 kV each, Bottom

to the single actuator case. However, there is only about a 3% difference in the lift. The big deficit comes from the drag. This is because the separation region reaches about 13% further upstream for the multiple actuator case. This increases the drag by nearly 11%. Because of this, there is no reduced voltage level option observed when using multiple, steady actuators compared to a single, steady actuator.

5.2.4. Investigation of Flow Control with Multiple, Unsteady Actuators

Similar observations made for the single, unsteady actuator cases can also be made for the multiple, unsteady actuator cases. The unsteady actuators do not provide significant improvement compared to steady actuators. The pulsing effect does not induce a vortex shedding process as a region of separation remains attached to the trailing edge. Like with the single, unsteady actuators, multiple, unsteady actuators are able to keep the separation confined to the trailing edge which does provide significant enhancement in aerodynamic performance (L/D), though the same improvement as single, steady actuator cases is not seen. L/D values for each to the analyzed configurations are given in Table 5. Figure 18 shows periodic behavior for a multiple actuator configuration compared to a single, steady actuator of the same time averaged body force. While drag value is approximately the same as seen in Figure 18, the suction near the leading edge is not as substaintial compared to the single, steady actautor case. As with the multiple, steady actuators, there is no observed reduced voltage level option savings when using multiple, unsteady acutuators compared to a single, steady actuator.

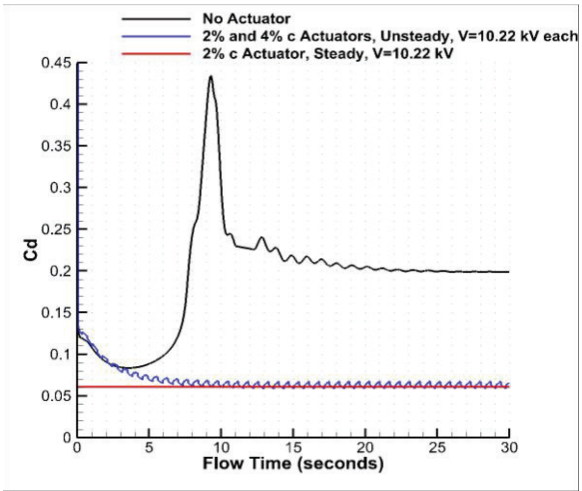

Figure 18. Drag Coefficient vs. Flow Time for Multiple, Unsteady Actuators at 15 Degrees Angle of Attack, V = 10.22 kV each, DC = 50%

5.2.5. Summary of the Results

<u>The Effect of Plasma Actuator Location:</u> Overall, similar trends are observed as with the laminar separation cases, most importantly with regards to actuator placement. Even though all of the actuator configurations are capable of providing significant improvement to the aerodynamic performance of the airfoil, the most efficient and effective approach is to ensure that the actuator is located upstream of any separation that may be present in the flow. The results in Table 4, as well as the figures throughout this section suggest that it is possible to the control separated flow coming from the trailing edge using leading edge actuators. As long as the added momentum from the plasma actuator is sufficient enough to keep the separation region from moving forward over the maximum thickness of the airfoil, then the significant loss in aerodynamic performance associated stall conditions (substantially decreased lift and increased drag.) This conclusion explains why a significant increase in L/D (Table 4) is observed of nearly every case investigated. Each configuration has the ability to suppress the separation region given a high enough voltage input. The results also indicate that the actuator(s) nearest to the leading edge provides the most improvement in L/D. This is due to the increase in suction near the leading edge. While all the configurations can reduce the separation region

size thereby reducing the form drag, the actuator nearest to the leading edge causes the greatest increase in the suction resulting in improved lift by the airfoil. An actuator placed at the leading may, in fact, improve L/D beyond that seen in this study. This would not only be due to the ability of the actuator to reduce the separation zone size (as seen for all the configurations in this study), but also due to the ability to significantly reduced the pressure in the suction region thereby increasing lift.

The Effect of Steady vs. Unsteady Operation: In general, the steady state actuators outperform unsteady actuators both in terms of effectiveness and efficiency as even unsteady actuators with the same time averaged force magnitude as a single actuator cannot provide the same level of aerodynamic improvement. This is quite the opposite that what was observed for the control of the laminar separation bubbles, where the unsteady actuator was, in every case, more effective and efficient in improving the aerodynamic performance compared to a steady actuator at the same time averaged force magnitude. This is because of the type of separation which is a trailing edge separation as opposed to a leading edge separation near the location of the actuators. Also, note that the most improvement was achieved from using the actuator nearest to the leading edge as this provides the most improvement in the suction and, in turn, lift.

The Effect of Multiple Plasma Actuators: Overall, there is not a substantial gain to using the multiple actuator configurations investigated in this study (multiple actuators in the leading edge region.) For multiple, steady actuators the reduction in the separation region size is similar for a single, steady actuator with the same total, additive, body force. However, the improvement in the suction is not as substantial as the as half of the added momentum is further away from the leading edge. The same effects are seen for multiple, unsteady actuators compared to a single, unsteady actuator where the disturbances generated by the pulsing effect do suppress the separation region from covering the entire upper surface, however, the aerodynamic improvement is not as significant compared to a single, steady actuator at the same time averaged body force.

6. CONCLUSIONS

The primary objective of this study was to investigate and demonstrate the effectiveness of aerodynamic plasma actuators as a means of active flow control over airfoils for a range of angles of attack. This included analyzing two flow scenarios that are detrimental to aerodynamic performance: laminar separation bubbles at a low angle of attack and turbulent separation at stall conditions at a high angle of attack. Results were obtained for actuators operating in both steady and unsteady modes, as well as multiple actuator configurations.

For the laminar separation bubble cases, successful reduction in separation size was achieved resulting in as much as a 45% recovery of the lift to drag ratio. Results also indicate that with the use of a single, unsteady actuator the same, if not slightly more improvement could be achieved with as little as 25% of the body force magnitude of a single, steady actuator. In all cases, unsteady actuators provide as much as a 12% improvement over a single actuator at the same time averaged body force magnitude at a lower input voltage level. The improvement with the unsteady actuators is due to an induced, periodic vortex shedding process which prevents large scale separation from occurring. Similar trends are seen for the multiple actuator configurations (both steady and unsteady.) Nearly the same aerodynamic improvement is achieved for multiple actuator configurations as with steady actuator configurations at the same time averaged body force magnitude, with the same mode of operation.

Another important conclusion drawn from these results was the dependence on actuator location relative to the separation region. It was found that if the actuator was located inside the separation region, it may not be effective at all. If separation control can be achieved, it comes at a great cost in terms of required input voltage. The optimum location for an actuator would be just upstream of the separation location. This is where the usefulness of multiple actuator systems becomes clear. In a dynamic environment, the separation location may be changing, especially in laminar separated flows where the separation location propagates upstream with increasing angle of attack. In this case, a single actuator may not be able to control the flow separation across the range of angles of attack, both effectively and efficiently. Multiple actuator systems may also be useful in scenarios where a single actuator can only prevent separation for a short distance downstream. An array of actuators would allow for continuous propagation of the separation location downstream. This suggests that the use of multiple actuator configurations may be the most practical design for aerospace applications that operate in this flow regime.

For turbulent separated flow at stall conditions, similar trends were observed for single, steady actuators. For the cases studied, a recovery of the aerodynamic performance of the airfoil was achieved. This is primarily due to the suppression of the separation region towards the trailing edge as well as the increased suction on the leading edge. Multiple, steady actuators have a similar effect when compared to a single, steady actuator of the same additive body force. While the reduction in the separation region size may be the same between the two, the L/D enhancement is not as great for multiple, steady actuators as the suction on the leading edge is not as substantial.

However, the same improvement was not achieved with unsteady actuation, whether with a single actuator or multiple actuators for this case. While there is significant improvement compared to the uncontrolled case, that improvement is not as much as is achieved from steady actuators. This is because of the nature of the separation region, which originates in the trailing edge region rather than the leading edge. The same periodic vortex shedding seen with the laminar separated flows is not observed in this case. The unsteady actuator creates a periodic swelling and deflating effect on the trailing edge separation, but never causing detachment. In a case where the separation was coming from the leading edge (at a lower Reynolds number or with a different geometry) and the separation location was only being pushed slightly downstream by a single actuator, multiple actuators may prove to be an effective alternative to continuously move the separation location downstream as far as required to maintain attached flow.

ACKNOWLEDGEMENTS

The authors would like to thank the NASA Missouri Space Grant Consortium for supporting this work.

REFERENCES

[1] Suzen, Y. B., Huang, P. G., and Jacob, J. D., “Numerical Simulations of Plasma Based FlowControl Applications,” AIAA-Paper 2005-4630, 35th AIAA Fluid Dynamics Conference and Exhibit, Toronto, Ontario Canada.

[2] Huang, J., Corke, T. C., and Thomas, F. O., “Unsteady Plasma Actuators for Separation 1487.

[3] Benard, N., Bonnet, J. P., Touchard, G., and Moreau, E., “Flow Control by Dielectric Barrier Discharge Actuators – Jet Mixing Enhancement,” AIAA 2008-3878, *4th AIAA Flow Control Conference,* Seattle, Washington.

[4] Thomas, F. O., Alexey, K., and Corke T. C., “Plasma Actuators for Landing Gear Noise Reduction,” AIAA 2005-3010, *26th AIAA Aeroacoustics Conference,* Monterey, California.

[5] Corke, T. C., and Post, M. L., “Overview of Plasma Flow control: Concepts, Optimization and Applications,” AIAA-Paper 2005-563, *43th AIAA Aerospace Sciences Meeting and Exhibit,* Reno, Nevada.

[6] He, C., Corke, T. C., and Patel, M. P., “Plasma Flaps and Slats: An Application of Weakly Ionized Plasma Actuators,” *Journal of Aircraft,* Vol. 46, No. 3, 2009, pp. 864-873.

[7] Mabe, J. J., Calkins, F. T., Wesley, B., Taubert, L., and Wygnanski, I., “Single Dielectric Barrier Discharge Plasma Actuators for Improved Airfoil Performance,” *Journal of Aircraft,* Vol. 46, No. 3, 2009, pp. 847-855.

[8] Aholt, J., and Finaish F., “Active Flow Control Strategy of Laminar Separation Bubbles Developed over Subsonic Airfoils at Low Reynolds Numbers,” AIAA-Paper 2011-733, *49th AIAA Aerospace Sciences Meeting including the New Horizons Forum and Aerospace Exposition,* Orlando, Florida.

[9] Visbal, M. R., Gaitonde, D. V., and Roy, S., “Control of Transitional and Turbulent Flows Using Plasma-Based Actuators,” AIAA-Paper 2006-3230, *AIAA Fluid Dynamics and Flow Control Conference,* San Francisco, California.

[10] Tsubakino, D., Tanaka, Y., and Fujii, K., “Effective Layout of Plasma Actuators for a Flow Separation Control on a Wing,” AIAA-Paper 2007-474, *45th AIAA Aerospace Sciences Meeting and Exhibit,* Reno, Nevada.

[11] Corke, T. C., Post, M. L., and Orlov, D. M., “SDBD plasma enhanced aerodynamics: concepts, optimization and applications,” *Computers & Fluid,* Vol. 43, 2007, pp. 193-217.

[12] Shan, H., Jiang, L., and Liu, C., “Direct Numerical Simulation of flow separation around a NACA 0012 airfoil,” *Computers & Fluid,* Vol. 34, 2005, pp. 1096-1114.

[13] Enloe, C. L., McLaughlin, T. E., VanDyken, R. D., Kachner, K. D., Jumper, E. J., Corke, T. C., Post, M., and Haddad O., "Mechanisms and Responses of a Single Dielectric Barrier Plasma Actuator: Geometric Effects," *AIAA Journal,* Vol. 42, No. 3, 2004, pp.595-604.

[14] Shan, H., Jiang, L., Liu, C., Love, M., and Maines, B., "Numerical Study of Passive and Active Flow Separation Control Over a NACA 0012 Airfoil," *Computers & Fluid,* Vol. 37, 2008, pp. 975-992.

[15] *ANSYS FLUENT User Manual.*

[16] Barth, T. J., Pulliam, T. H., and Buning, P. G., "Navier-Stokes Computation for Exotic Airfoils," AIAA-Paper 1985-109, *23rd AIAA Aerospace Sciences Meeting,* Reno, Nevada.

[17] West IV, T. K., "Numerical Investigation of Plasma Actuator Configurations for Flow Separation Control at Multiple Angles of Attack," Master's Thesis, Missouri University of Science and Technology, 2012.

[18] Spalart, P. R., and Allmaras, S. R., "One-Equation Eddy-Viscosity Turbulence Models for Engineering Applications," AIAA-Paper 92-0439, *30th Aerospace Sciences Meeting and Exhibit,* Reno, Nevada.

[19] Lian, Y., and Shyy, W., "Laminar-Turbulent Transition of a Low Reynolds Number Rigid or Flexible Airfoil," AIAA Journal, Vol. 45, No. 7, 2007, pp. 1501–1513.

[20] Nichols, T. G., and Rovey, J. L., "Fundamental Process of DBD Plasma Actuators Operating at High Altitude," AIAA-Paper 2012-0822, *50th AIAA Aerospace Sciences Meeting including the New Horizons Forum and Aerospace Exposition,* Nashville, Tennessee.

[21] Porter, C. O., Baughn, J. W., McLaughlin, T. E., Enloe, C. L., and Font, G. I., "Temporal Force Measurements on an Aerodynamic Plasma Actuator," AIAA-Paper 2006-104, *44th AIAA Aerospace Sciences Meeting and Exhibit,* Reno, Nevada.